Development of extractive electrospray ionization ion trap mass spectrometry for *in vivo* breath analysis

Jianhua Ding,[ab] Shuiping Yang,[a] Dapeng Liang,[b] Huanwen Chen,*[ab] Zhuanzhang Wu,[b] Lili Zhang[a] and Yulin Ren*[a]

In metabolomics studies and clinical diagnosis, interest is increasing in the rapid analysis of exhaled breath. *In vivo* breath analysis offers a unique, unobtrusive, non-invasive method of investigating human metabolism. To analyze breath *in vivo*, we constructed a novel platform of extractive electrospray ionization (EESI) ion trap mass spectrometry (ITMS) using a home-made EESI source coupled to a linear trap quadrupole mass spectrometer. A reference compound (authentic *n*-octyl amine) was used to evaluate effects of systematically varying selected characteristics of the EESI source on signal intensity. Under the optimized working conditions, metabolic changes of human bodies were *in vivo* followed by performing rapid breath analysis using the multi-stage EESI-ITMS tandem mass spectrometry platform. For nicotine, a limit of determination was found to be 0.05 fg mL^{-1} ($S/N = 3$, $RSD = 5.0\%$, $n = 10$) for nicotine in aerosol standard samples; the dynamic response range was from $0.0155 \text{ pg mL}^{-1}$ to 155 pg mL^{-1}. The concentration of nicotine in the exhaled breath of a regular smoker was *in vivo* determined to be 5.8 pg mL^{-1}, without any sample pre-treatment. Our results show that EESI-ITMS is a powerful analytical platform to provide high sensitivity, high specificity and high throughput for semi-quantitative analysis of complex samples in life science, particularly for *in vivo* metabolomics studies.

Introduction

Metabolomics studies are of tremendous interest in multiple disciplines, especially in system biology,[1–4] drug discovery[5–7] and clinical diagnosis.[8–12] Techniques including NMR,[8,13–16] mass spectrometry,[11,17–23] chromatography[24,25] and optical spectros-copy[8,26–28] have been used for metabolomics studies. In contrast with the blossoming techniques, the samples for metabolomics are somewhat restricted to biofluids. Regardless of the source, biofluids originating from either animals or human beings, such as urine and blood/serum, are typical samples widely used for metabolomics studies,[1–12] providing plentiful chemical information to study metabolic processes. Urine rather than blood is much more convenient to be used, since urine is non-invasively available. However, privacy is not ideally respected in certain cases (*e.g.*, sport doping analysis[29–31]) where urine samples should be authentically collected to avoid sample manipulation.

Alternatively, exhaled breath can be used as samples for metabolomics studies.[11,32–38] Breath contains fewer matrices (*e.g.*, salts, water, *etc.*) than urine or blood. This eases breath analysis for most techniques, obviating tedious sample collection and pretreatment protocols. Obviously, breath is non-invasively available and continuously accessible, while the patient's privacy is perfectly respected. Besides the abovementioned advantages, breath serves as a short cut for metabolites to come out of a body. Studies have shown that both volatile and non-volatile metabolites can be detected in exhaled breath.[11,35] Therefore, it is highly desirable to use exhaled breath as a sample for metabolomics studies.

Decades ago, breath condensate analysis (BCA)[33,34,36–40] was proposed for detection of compounds present in exhaled breath. Usually, exhaled breath is pre-concentrated using liquid helium, thus the volatile compounds are separated from the rest of the major components (*e.g.*, water, nitrogen) of breath at a temperature lower than the melting point of nitrogen. In such a case, water-soluble compounds such as urea and glucose are not detectable, because these compounds cannot be released from the ice. Normally, extremely volatile compounds (*e.g.*, CO_2, NO, NO_2, *etc.*) are favorably detected in BCA.[33,34,41,42] Similar to BCA, many other techniques[43–49] have focused on detection of relatively small molecules (*i.e.*, MW $\leq$ 200 Da) in breath. Recently, semi-volatile and water-soluble compounds, including urea, glucose, *etc.*, have been sensitively detected from exhaled breath directly using newly developed extractive electrospray ionization (EESI) time-of-flight mass spectrometry,[11] showing that the metabolic response of human bodies can be followed *in vivo* by profiling the chemical mass spectral fingerprints. In EESI, which was introduced as a variant of ESI in 2006,[50] neutral analytes present in complex matrices are dispersed in a spatial cross section formed between a sample plume and an electro-spray beam; thereby the analytes undergo interactions and collisions with the primary ions produced by electrospraying pure solvent (*e.g.* acetic acid/methanol water solution), and then ionized for further mass spectral analysis.[11,12,21,23,50–53] Apparently, ion suppression is reduced in EESI by distributing the

College of Chemistry, Jilin University, Changchun, 130021, P.R. China. E-mail: ylren@jlu.edu.cn
Department of Applied Chemistry, East China Institute of Technology, Fuzhou, 344000, P.R. China. E-mail: chw8868@gmail.com; Fax: (+86) 0794-8258320; Tel: (+86) 0794-8258320

matrices over a relatively wide section in a 3-dimensional space. Clean solvents, such as a methanol–water solution, can be used to maintain a constant ion yield in ESI for a long time. This ensures that stable signals of analytes in complex matrices can be maintained for more than 7 hours in EESI-MS.[22,50] Another unique feature of EESI is that the neutral samples (*e.g.* biological subjects) are safely isolated from any high voltage or direct bombardment by charged particles, thus living objects can be conveniently analyzed *in vivo*, with neither sample pre-treatment nor chemical contamination. The concept of *in vivo* breath analysis has been demonstrated by using EESI implemented in a commercially available quadrupole time-of-flight mass spectrometer (QToF-MS).[11] Previous preliminary results proved that non-volatile compounds are detectable in breath, clearly showing that metabolic changes of a human body can be promptly followed by profiling the chemical mass spectral fingerprints of exhaled breath samples.

Although it is easy to perform EESI in a commercial QToF-MS instrument, the wide application of the EESI-QToF-MS is restricted by the lack of flexibility for optimization of the EESI source and by the limited capability for multiple-stage mass spectrometry. Without sample pre-treatment (*i.e.*, matrix separation), tandem MS capability is strongly required for explicative detection. Among the many types of analyzers available, ion trap mass analyzers hold advantages such as high sensitivity, relatively low cost and easy availability, and provide the most competitive capability of performing multiple-stage mass spectrometry.[8,13,20,27]

Motivated by implementing tandem mass spectrometry for breath analysis, a home-made EESI source was coupled to a commercial ion trap mass spectrometer, resulting in a versatile platform for *in vivo* analysis of human breath. The novel EESI tandem MS platform was systematically characterized using *n*-octyl amine as a reference compound. As a demonstration, mass spectral fingerprints of human breath were *in vivo* recorded from volunteers. Tandem mass spectra of species of interest were recorded to elucidate the molecular structure of the analytes.

Under the optimized conditions, the LOD of nicotine was found to be 0.05 fg mL^{-1}, and quantitative analysis of nicotine in the exhaled breath of smokers was also achieved, showing a linear dynamic range of 5 orders of magnitude.

Experimental

Experimental setup

Experiments were carried out using a LTQ-XL mass spectrometer (Finnigan, San Jose, CA, USA) equipped with a home-made EESI source. The principle and basic configurations of an EESI source were previously illustrated for rapid analysis of liquid samples.[22,50,54,55] Briefly, the EESI source described here was constructed for *in vivo* breath analysis, with enhanced specificity by using tandem mass spectrometry. As schematically shown in Fig. 1, the EESI source consists of two channels: one for sample introduction, and the other for generation of reagent ions by electrospraying matrix-free solvents. To construct a simple ESI source, a long piece of small capillary (ID 0.10 mm, OD 0.15 mm, Agilent Technologies Co., Ltd., USA) passed through a union tee tube (Swagelok, OH, USA) to guide the solvent mixture (*e.g.*, aqueous acetic acid solution) to the electrospraying site; and a relatively big capillary (ID 0.25 mm, OD 0.40 mm, Agilent Technologies Co., Ltd., USA) was coaxially inserted between the inner wall of the tee tube and the small capillary to introduce sheath gas for the electrospray. The length of the big capillary was no more than half length of the tee tube. The geometry of these two capillaries was carefully arranged such that the inner capillary protruded and was exposed to air for about 0.5–1 mm, and that the outer capillary was open inside the tee tube. A gas line was mounted to the union tee at the unoccupied end such that pure nitrogen gas (purity ≥ 99.99%) came out *via* the rift between the outer capillary and the inner capillary to assist the solvent nebulization. A high voltage (*e.g.*, +3 kV) was applied to the pure solvent inside the inner capillary to sustain a reliable ESI process. For liquid samples, the sample plume was neutrally
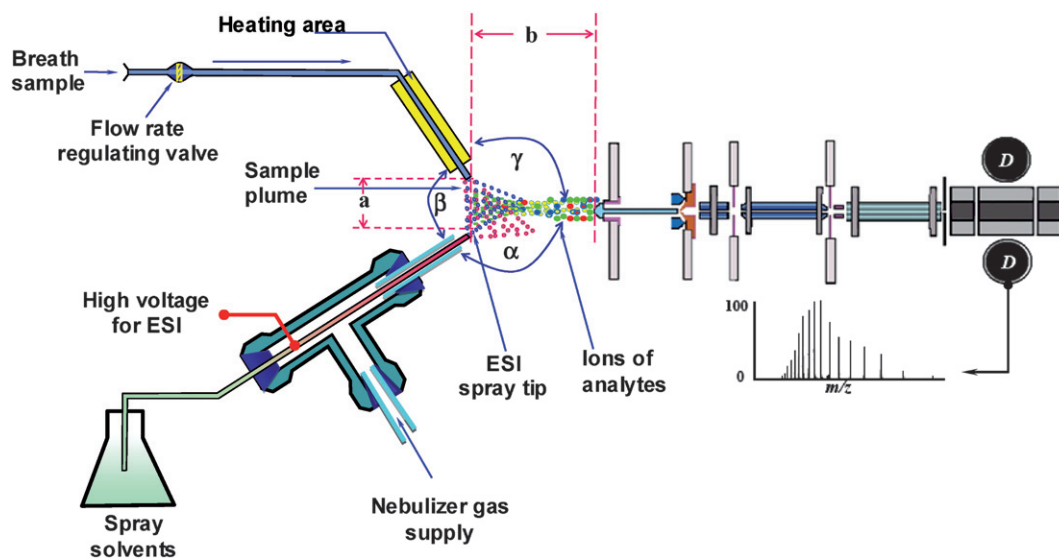
Fig. 1 Schematic illustration of EESI-LTQ-MS for *in vivo* breath analysis. Note that the distances *a*, *b* and the angles *α*, *β*, *γ* were experimentally optimized to achieve better sensitivity. The dimensions are not proportionally scaled.

Table 1 Calculated gas-phase nicotine concentrations obtained using nicotine working solutions[a]

c_l/μg.mL^{-1}	0.010	0.025	0.050	0.075	0.10	0.25	0.50	0.75	1.0	2.5	5.0	7.5	10	25	50	75	100
c_g/pg.mL^{-1}	0.0155	0.03875	0.0775	0.11625	0.155	0.3875	0.775	1.1625	1.55	3.875	7.75	11.625	15.5	38.75	77.5	116.25	155

[a] c_l is the liquid concentration of nicotine working solution; c_g is the corresponding concentration of nicotine in the nicotine aerosol. The experiment was done using the setup shown in Fig. 2, under 25 °C; the total pressure inside the flask was 1.10×10^5 Pa.

generated in the sample introduction channel, which was of the same geometry and structure of the electrospray channel. The two channels were arranged in front of the LTQ-MS instrument to form a special cross section between the MS inlet of the instrument, the electrospray channel and the sample introduction channel. For aerosol samples such as exhaled breath, the sample nebulization channel was carefully replaced by a piece of Teflon tube (ID 3 mm, OD 3.5 mm), but the configuration and position were unchanged. Passing through a flow-rate-regulating valve (a gift from Shanghai Spectrum Ltd, Shanghai), the exhaled gas was blown into the Teflon tube, and then directed to the EESI source (shown in Fig. 1). To facilitate the nebulization process of exhaled gas and avoid breath condensation, the Teflon tube was heated to 100 °C at the end placed closely to the electrospray beam. In the EESI source, the neutral analytes underwent numerous collisions with the charged particles generated by the electrospray channel. During these collisions, on-line droplet–droplet extraction occurred, allowing continuous extraction of interesting compounds and subsequent ionization of neutral analytes. The analyte ions were then introduced into the LTQ mass analyzer for mass analysis through the ion guide system of the LTQ-MS instrument. The EESI assembly was amounted on a 3-D adjustable stage. The distance (a) between the two channels of the EESI source and the distance (b) between the tips of the EESI source and the MS inlet were optimized to be 7 mm and 10 mm, respectively. The angle (α) between the electrospray channel and the MS inlet of the LTQ-MS instrument and the angle (β) between the two channels of the EESI source were set to be 134° and 77°, respectively. Thus, the angle (γ) was determined to be 149°. These angles were adjustable before optimization. The LTQ-MS instrument was running in positive ion detection mode. The temperature of the heated capillary of the LTQ-MS was maintained at 100 °C to avoid any significant thermal dissociation of the analytes ions. The voltages of default values were used for the heated capillary, the tube lenses, the conversion dynode, the detectors, *etc.* Further optimization was not performed.

All the full scan mass spectra were recorded using Xcalibur® software of the LTQ-MS instrument with an average time of 1.5 min. The precursor ions of interest were isolated using a mass window of 1.0 mass/charge unit. Collision-induced dissociation (CID) experiments were performed by applying 18–30% (arbitrary units defined by the LTQ instrument) collision energy for 30 ms to the precursor ions. MS^n spectra were collected with a recording time more than 1.5 min if necessary. Compounds of interest were identified using MS and CID data matching of the unknown compounds against authentic standards.

Materials and reagents

Chemicals such as *n*-octyl amine (analytical reagent grade, Sinopharm Chemical Reagent Co., Ltd, Beijing, China), nicotine (analytical reagent grade, Sigma–Aldrich. Inc, St Louis, MO, USA), methanol (HPLC grade, Fisher Scientific, Fair Lawn, NJ, USA), acetic acid (HPLC grade, Sinopharm Chemical Reagent Co., Ltd, Beijing, China) were directly used without further pretreatment, except for dilution with pure water (or methanol) if necessary. The water used was deionized water, which was provided by the chemistry department facility.

A working solution of *n*-octyl amine (10 ng mL^{-1}), prepared by diluting *n*-octyl amine stock solution (1 mg mL^{-1}) with methanol, was directly infused by using a syringe pump (5 μL min^{-1}) to the sample introduction channel of the EESI source. A stock solution of nicotine (1 mg mL^{-1}) was prepared using water as the solvent. 17 individual solutions of nicotine (concentration varied from 0.01 to 100 μg mL^{-1}, Table 1) were carefully prepared by properly adding water into the nicotine stock solution. These diluted nicotine solutions were used as standard working solutions of nicotine to acquire a calibration curve.

Cigarettes were purchased from a local store and used as usual without any pre-treatment. Volunteers for nicotine experiments were chosen from healthy adults, including one male regular smoker (28 years old with 5 years smoking experience), one male non-smoker (28 years old) and one female non-smoker (39 years old). All volunteers maintained their normal daily life and diet during the experiments, no special care was taken for the volunteers. All the breath samples were directly blown into the abovementioned Teflon tube with a clean, fresh mouth interface for each volunteer. Note that the experimental and safety issues have been addressed according to local legislation, but extra caution should be taken for analysis of breath donated from an unknown subject to prevent any potential infection.

Procedure to prepare standard gas-phase nicotine samples

One of the nicotine working solutions (250 mL) was added into an Erlenmeyer flask (500 mL, BRAND GMBH + CO KG, Germany), which was air-tightly sealed with a Teflon blocker. A Teflon gas line (ID 3 mm, OD 3.5 mm) passing through the Teflon blocker was dipped into the solution, allowing a gap (*ca.* 3 mm) between the end of the gas line and the surface of the flask. Another Teflon tube (ID 3 mm, OD 3.5 mm) inserted into the flask introduced the headspace of the solution into the EESI source. Two toggle valves (Swagelok OH, USA) were installed to the two gas lines (as shown in Fig. 2), respectively, to control the gas flow. Before the working solution was added, the two valves were closed. Once the working solution was added into the sealed flask, the valve 1 was opened and the nitrogen gas filled the flask until the pressure was balanced by the nitrogen gas tank to be 1.10×10^5 Pa. The two valves were closed for about 30 min. This allowed the phase equilibrium to be reached between the headspace, which contained water, nicotine and air,
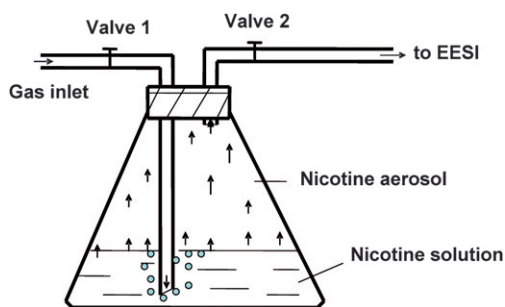
Fig. 2 The Erlenmeyer flask containing nicotine solution. The temperature of the container was 25 °C, and the pressure inside the flask was 1.10×10^5 Pa.

and the nicotine working solution. The valve 2 was then opened, directing the nicotine aerosol mixture to the EESI source for ionization. The data for making the nicotine calibration curve was recorded using SIM operation model of the LTQ-MS instrument. Note that the experiments were done at 25 °C. Since the nicotine solutions for these experiments have been extremely diluted, the solute of the solution follows Henry's Law. Meanwhile, the gas-phase material of the solution follows Boyle's Law and Gay–Lussac's Law, because the temperature is not too low (25 °C) and the pressure is not too high (1.10×10^5 Pa).

The gas-phase nicotine concentration of a given standard solution can be calculated as below

$$c_g = y_n c_v \tag{1}$$

where c_g is the mass concentration (g L^{-1}) of nicotine in water vapor; y_n is the molar fraction of nicotine in the gas phase; c_v is the mass concentration (g L^{-1}) of 1 molar pure nicotine vapor under the experimental conditions (298 K, 1.10×10^5 Pa).

$$c_v = \frac{m_n}{V} \tag{2}$$

where m_n is the molar mass of nicotine; V is the molar volume of nicotine under the experimental conditions (298 K, 1.10×10^5 Pa).

According to the Clapeyron equation, at a temperature of 25 °C and pressure of 1.10×10^5 Pa, the volume of 1 molar nicotine vapor can be approximately calculated as below:

$$
\begin{aligned}
V &= \frac{nRT}{P_t} \\
&= \frac{1 \text{ mol} \times 8.314 \text{ J K}^{-1} \text{ mol}^{-1} \times 298 \text{ K}}{1.10 \times 10^5 \text{ Pa}} \approx 22.5 \times 10^{-3} \text{ m}^3 \\
&= 22.5 \text{ L}
\end{aligned}
$$

According to Dalton's partial pressure law, the mole fraction of nicotine in the gas phase is equal to the ratio of its partial pressure to the total pressure, that is

$$y_n = \frac{P_n}{P_t} \tag{3}$$

where P_n is the pressure of nicotine in the gas phase; P_t is the total pressure in the gas phase.

According to Henry's Law, the partial pressure of nicotine in the gas phase is directly proportional to the concentration of nicotine in solution, that is

$$P_n = k_n x_n \tag{4}$$

where k_n is Henry's constant of nicotine (as reported,[56,57] k_n of nicotine under the molar fraction per unit is 213 Pa at 25 °C); x_n is the molar fraction of nicotine in the working solution, and

$$x_n = \frac{c_1/m_n}{d_w/m_w} = \frac{c_1 m_w}{m_n d_w} \tag{5}$$

where c_1 is the nicotine concentration of the working solution; m_n is the molar mass of nicotine; m_w is the molar mass of water; d_w is the density of water at the temperature for the experiments.

Entering eqn (4) and eqn (5) into eqn (3), y_n is given as below:

$$y_n = \frac{k_n \dfrac{c_1 m_w}{m_n d_w}}{P_t} = \frac{k_n m_w}{P_t m_n d_w} c_1 \tag{6}$$

Entering eqn (2) and eqn (6) into eqn (1), the concentration of nicotine in the gas phase can be calculated using the equation below:

$$c_g = \frac{k_n m_w c_1}{P_t m_n d_w} \frac{m_n}{V} = \frac{k_n m_w}{P_t V d_w} c_1 \tag{7}$$

Given,

$k_n = 213$ Pa; $P_t = 1.10 \times 10^5$ Pa; $m_w = 18$ g mol^{-1}; $V = 22.5$ L mol^{-1}; $d_w = 1$ g mL^{-1}

and entering these into eqn (7), then

$$c_g = \frac{213 \text{ Pa} \times 18 \text{ g mol}^{-1}}{1.10 \times 10^5 \text{ Pa} \times 22.5 \text{ L mol}^{-1} \times 1 \text{ g mL}^{-1}} c_1 \approx 1.55 \times 10^{-6} c_1 \tag{8}$$

Consequently, the gas-phase concentration of nicotine samples was calculated using eqn (8), as shown in Table 1.

Results and discussion

Optimization of EESI source

Initially, the EESI source was characterized using an *n*-octyl amine solution (10 ng mL^{-1}) before the breath analysis was performed. The experimental parameters such as the electrospray voltage, the sample flow rate, the electrospray solution composition and its flow rate, the nebulizer gas pressure, the temperature of the heated capillary, and the geometry including the angles (α, β) and the distances (a, b) of the EESI source were experimentally optimized.

Electrospray voltage

In a typical EESI experiment, analyte molecules are neutrally sprayed into the electrospray plume, where micro liquid droplet–droplet extraction/ionization occurs, providing an extraction-based process for ion formation.[22,50,55] In this study, the working conditions were selected by optimizing the signal intensity of
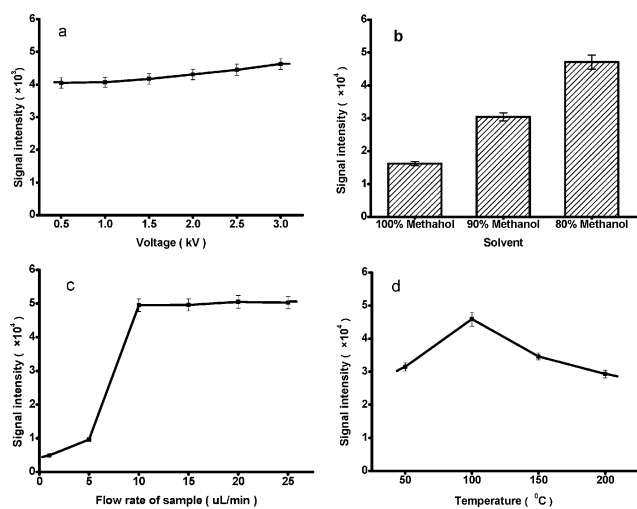
Fig. 3 Effects of the EESI working conditions on the signal intensity levels of analytes. a: Effects of the electrospray high voltage; b: effects of the composition of the electrospray solution; c: effects of the sample infusion rate; d: effects of the temperature of the heated capillary. The error bars indicate 5% of the averaged signal.

n-octyl amine. Fig. 3a shows the effect of the electrospray voltage on the signal intensity level of protonated *n*-octyl amine (m/z 130). The data show that, within a relatively wide range (1–3 kV), the fluctuation of voltage had a minimal effect on the signal intensity of *n*-octyl amine (m/z 130). This indicates that primary ions were constantly generated by electrospraying methanol solution; even using a low electrospray voltage. Usually, a low signal level can be expected when water solution is electrosprayed at low voltages (*e.g.*, 1 kV), probably because water has a relatively large surface tension and thus results in poor ionization efficiency. Therefore, the stable signal observed here was ascribed to the utilization of methanol solvent, which generated the reagent ions constantly in the ESI process due to the low surface tension.[58] To accelerate the reagent ions generated in the electrospray process, a high voltage (*e.g.* ≥ + 4 kV) was used in previous studies.[11,12,21,50] However, a corona discharge occurring between the two channels of the EESI source was observed if a voltage higher than 3.5 kV was directly applied to the electrospray ionization, probably because a voltage higher than 3.5 kV was too much under the experimental conditions. Thus, the electrospray voltage was set to be 3 kV to avoid any discharge in this study.

Infusion rate of reagent solution

Applying a high voltage of 3 kV for the electrospray in this study, it was found that a stably high level signal of *n*-octyl amine was detected when the methanol solvent was electrosprayed with infusion rate varied from 1 μL min⁻¹ to 20 μL min⁻¹. Because methanol was very volatile and easy to be desolvated under the experimental conditions, a high infusion rate (*e.g.*, 20 μL min⁻¹) could be used. However, a signal drop was observed when the infusion rate of pure methanol exceeded 50 μL min⁻¹. When the spray solution contained a high content of water (60%, v/v), the signal intensity started to decrease when the solution infusion rate was more than 10 μL min⁻¹. These findings indicate that

sufficient desolvation of the primary ions generated by the ESI channel leads to a good signal of analytes in the EESI process. Certainly, acids help to generate protons in ESI. When an acetic acid water solution (10–20%) was electrosprayed at 2–5 μL min⁻¹, a high level signal of *n*-octyl amine was obtained. For the following experiments, the electrospray solvent was infused at 5 μL min⁻¹.

Sheath gas pressure for electrospray

The pressure of the ESI sheath gas affected the signal levels. Below a critical pressure of 1.4 MPa, the higher pressure of the sheath gas used, the higher level of the signal was observed. This was probably due to a better desolvation achieved by using a high sheath gas flow. The signal level was sustained when the sheath gas pressure varied from 1.4 MPa to 2.0 MPa. The analyte intensity decreased significantly (≥20%) when the sheath gas pressure exceeded 2.1 MPa, which might arise from the serious disturbance of the online extraction/ionization process by the extremely fast expansion of the gas flow. Thus, the sheath gas pressure was set at 1.7 MPa to generate good signals for the following experiments.

Composition of the electrospray solvent

EESI usually produces protonated/deprotonated molecules as signals for detection in positive/negative ion detection mode. As reported in a previous study,[11] analytes in breath are readily protonated in EESI to yield mass spectral fingerprints of components in the breath sample. Therefore, a positive ion detection mode was also employed in the current work. Usually, the sample solution is acidified by adding acetic acid or formic acid to facilitate proton generation in positive electrospray ionization process. However, most samples, especially biological samples (*e.g.*, proteins), tolerate a small amount of acid (*ca.* 0.05%) before being denatured. Taking advantage of the fact that the sample is separated from the electrospray process in EESI, it is convenient to investigate the effects of high acid content of the spray solution on the signal level of analytes. As shown in Fig. 3b, acetic acid–methanol solutions produce signals of *n*-octyl amine better than other solvents, such as pure methanol or basic solvents (data not shown). Comparing to the signal level obtained using pure methanol, the signal level was increased about 1.7 and 2.7 times when the content of acetic acid was 10% and 20%, respectively. With a further increasing of the acetic acid content in the spray solution, a slight improvement of the signal intensity (≤3 times) was observed (data not plotted), probably because the proton yield reached its maximum under the experimental conditions. However, a smell of acetic acid was found when acetic acid–methanol solutions of higher concentrations (≥30%) were electrosprayed at a flow rate of 5 μL min⁻¹. Therefore, the solution of metanol–acetic acid (4 : 1 v/v) was selected as the electrospray solution for the following EESI experiments.

Sample flow rate

Under the given conditions, the signal intensity level of *n*-octyl amine was mainly affected by the sample infusion rate and by the

nebulizer gas pressure used to produce the sample plume. While the sample nebulizer gas pressure was kept at 1.7 MPa, the signal intensity increased rapidly when the sample flow rate was raised from 1 μL min⁻¹ to 10 μL min⁻¹; the signal sustained the same level while the sample flow rate was increased to 25 μL min⁻¹ (as shown in Fig. 3c). Although the detailed mechanisms of EESI process have not been systematically studied, it is expected that gas-phase collisions and charge exchange play key roles for extractive electrospray ionization. Theoretically, better desolvation of the neutral analytes (i.e. higher nebulizer gas pressure) will result in a better signal. From a point view of desolvation, a lower sample infusion rate should be used to achieve a better signal in EESI. However, for a given sample solution, a low sample infusion rate reduces the total amount of analytes deliverable for ionization. This explains the signal enhancement with the infusion rate from 1 μL min⁻¹ to 10 μL min⁻¹. The analyte signal maintained the same level even when the sample infusion rate reached 25 μL min⁻¹. This was most likely due to a saturation of analytes to the reagent ions (e.g., protons). Under the experimental conditions, a signal decline was noticed when the sample infusion rate surpassed 35 μL min⁻¹; and the higher the sample infusion rate, the more profound the decline was. In all likelihood, this was due to insufficient desolvation of the analytes. For breath samples, the aerosol of the analytes was produced by the lung. However, it can be expected that the regulation of breath flow from different individual should be beneficial for quantitative analysis of certain compound in breath. For further optimization of the EESI source, the sample solution was infused at a flow rate of 10 μL min⁻¹.

## Temperature of the heated capillary

Heating the capillary eases the desolvation process of the charged droplets,[58] resulting in a better yield of analyte ions. It was found that the ion current of analyte ions increased slightly when the temperature of the heated capillary increased from 50 °C to 100 °C (as shown in Fig. 3d). However, the signal level decreased slightly when the heated capillary was baked up to 150 °C, probably because that under such a high temperature, the heat-induced-pyrolysis of the protonated analyte (e.g., n-octyl amine) occurred inside the hot capillary. Generally, most compounds in breath are metabolites of the human body. Theoretically, these compounds will probably dissociate quickly under a high temperature environment. Therefore, the heated capillary was maintained at 100 °C for the following experiments.

Optimization of the geometry of EESI

The unique design of EESI isolates the generation of reagent ions from the sample by using two separated channels (shown in Fig. 1). The flexible configuration of EESI makes it applicable to customize the angles (i.e., α, formed between the electrospray channel and the axial of the MS inlet; β, formed between the electrospray channel and the sample introduction channel; γ, formed between the sample introduction channel and the axial of the MS inlet) and the distances (a, between the tip of the electrospray channel and the tip of the sample introduction channel;

b, between the tip of the MS inlet and the front end of the EESI source) to meet the specific requirements of different applications. For example, it was found that angle $\alpha = \gamma = 150°$, $\beta = 60°$ while $a = 2$ mm and $b = 10$ mm are generally good for most applications to reach the best sensitivity; however, in cases where extremely dirty matrices are involved, the angle $\gamma \leq 90°$ is recommended to be set prior to other settings to achieve a good long term stability. For analysis of a relatively clean sample (e.g., breath), the α angle was tuned to be 134° with priority. This prevented shooting at the MS inlet capillary with a large amount of neutral molecules ejected from the electrospray channel. While the angle α was kept at 134°, β was optimized to be 77° by achieving the highest signal level of n-octyl amine. Under the given conditions, it was found that the signal level of the analyte was sensitive to the change of the angle β, especially when the angle β was less than 77° (as shown in Fig. 4a). The highly stable signal intensity was likely to be achieved by enabling efficient online micro extraction/ionization occurring between the charged droplets created by the electrospay and the neutral droplets of the sample aerosol. So far, it is still difficult to fully describe the mechanism of how the angles affect the signal intensity, because the interactions happening between the plumes generated by the two channels of EESI and the vacuum field created by the MS inlet was very complicated to describe in detail.

In our experiments, the signal intensity level was not significantly changed when the distance a was changed from 2 mm to 8 mm. This was probably due to the special section formed between the two spray channels and the MS inlet. The 3-dimensional section was of a relatively large size, in which the charge transfer reaction was completed with sufficient efficiency and could not be disturbed by a varying of the distance a. Therefore, prior to optimization of the distance b, the distance a was set to be 7 mm to avoid potential discharge. As shown in Fig. 4b, the strongest signal of analyte was detected while the distance b was 10 mm. A lower signal level was observed when the distance b was much less or more than 10 mm. The signal drop when the distance b was much less than 10 mm was because of insufficient desolvation since the retention time of the ions was not long enough. The desolvated ions pass through some distance before they come into the vacuum of the LTQ-MS instrument, surviving numerous collisions at atmospheric pressure. During the transportation, bared ions might quench quickly at atmospheric pressure. Consequently, a signal drop took place if the ions were required to pass through a distance
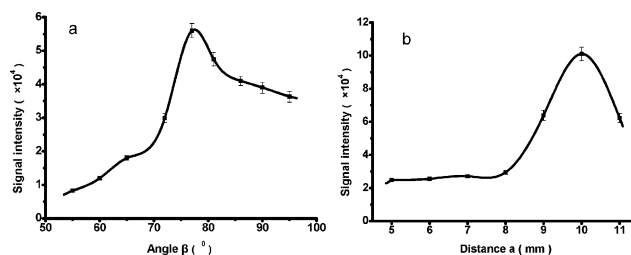
Fig. 4 Optimization of the geometry and configuration of the EESI source. a: Effects of the angle β on signal intensity levels; b: effects of the distance a on signal intensity levels. The error bars indicate the 5% of the averaged signal.

longer than 10 mm. Therefore, the distance b was set to be 10 mm for all the experiments.

EESI-MS spectra of exhaled breath

Breath is exhaled from the lung, which is directly associated with circulatory systems and is closely located to the heart and liver. Theoretically, components of breath carry molecular information correlating with metabolic processes of all these important organs. Furthermore, breath is the earliest non-invasively available sample to track the metabolic response caused by external compounds such as drugs. For example, swallowed pharmaceutical compounds enter blood in the digestive tract, and reach the liver—which is a chemical plant responsible for many metabolic processes—*via* the hepatic portal venous system, and then arrive at the lung by passing through the heart. Therefore, the signal of oral-taken drugs appears in breath earlier than in urine samples, which undergoes further body circulation and urinary bladder stock (several hours). Thus, it takes a much longer time to observe the metabolic response by using urine rather than breath as the sample.

Under the optimized experimental conditions, mass spectral fingerprints of breath were recorded using the LTQ-MS instrument from several volunteers, who were asked to directly breathe at a fairly similar rate into the EESI source for fast ionization. Similar to the previous results[11] obtained with EESI-QToF-MS, bunches of peaks were detected in a single full scan mass spectrum, providing informative mass fingerprints either in a low mass range (*e.g.*, *m/z* 20–200) or in a relatively high mass range (*e.g.*, *m/z* 200–1500). This was in good agreement with previous findings that compounds in exhaled air, even the relatively large molecular weight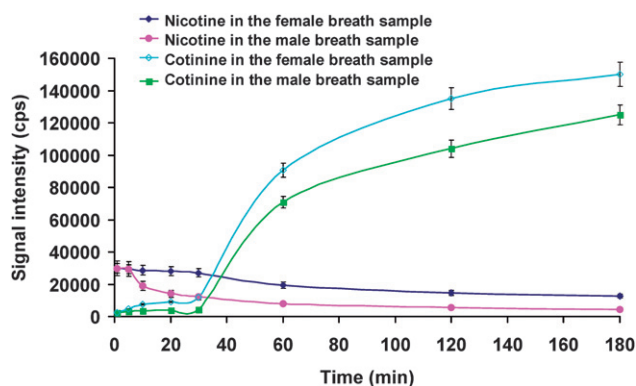 species, can be *in vivo* sampled for rapid detection by EESI-MS.[11] Experiments showed that as long as a sample is properly supplied to a normally functional EESI source, a mass spectral fingerprint is always straightforwardly recordable from an exhaled breath.

To simplify the comparison between mass spectra, mass spectral fingerprints recorded within the mass range from *m/z* 50 to *m/z* 800 are representatively shown in this study. The mass spectral fingerprints obtained from a male non-smoker volunteer are shown on the left panel of Fig. 5, while those recorded from a female non-smoker are shown on the right panel of Fig. 5. Among numerous mass spectral peaks in the mass spectrum collected from the breath before smoking, abundant peaks were detected at *m/z* 78, 83, 263, 279, 338 (as shown in Fig. 5a), confirming that the newly constructed EESI-LTQ-MS based on a home-made EESI source was capable of profiling metabolites in breath without any sample pre-treatment. No signal was detected for nicotine (MW 162), a well known bioactive compound in cigarettes, at *m/z* 163 from breath samples donated by the male non-smoker. After the volunteer smoked one dose of cigarette (nicotine content was 1 mg per dose) outside the lab room where the EESI experiment was implemented, however, nicotine was detected as protonated molecules at *m/z* 163 (as shown in Fig. 5b). The successful detection of nicotine was confirmed by using multiple-stage mass spectrometry against data matching using authentic nicotine as a reference compound (discussed in next section). Besides the signal of nicotine, many changes in terms of both signal intensity and peak density were found in the mass spectrum recorded after smoking. For instance, peaks such as *m/z* 80, 94, 122, 163, 236, 360 and *m/z* 597 showed up with remarkably increased intensity levels in Fig. 5b. In the zoomed view, it is clear that the peak density in Fig. 5b, particularly within the mass range of *m/z* 50–200, is much higher
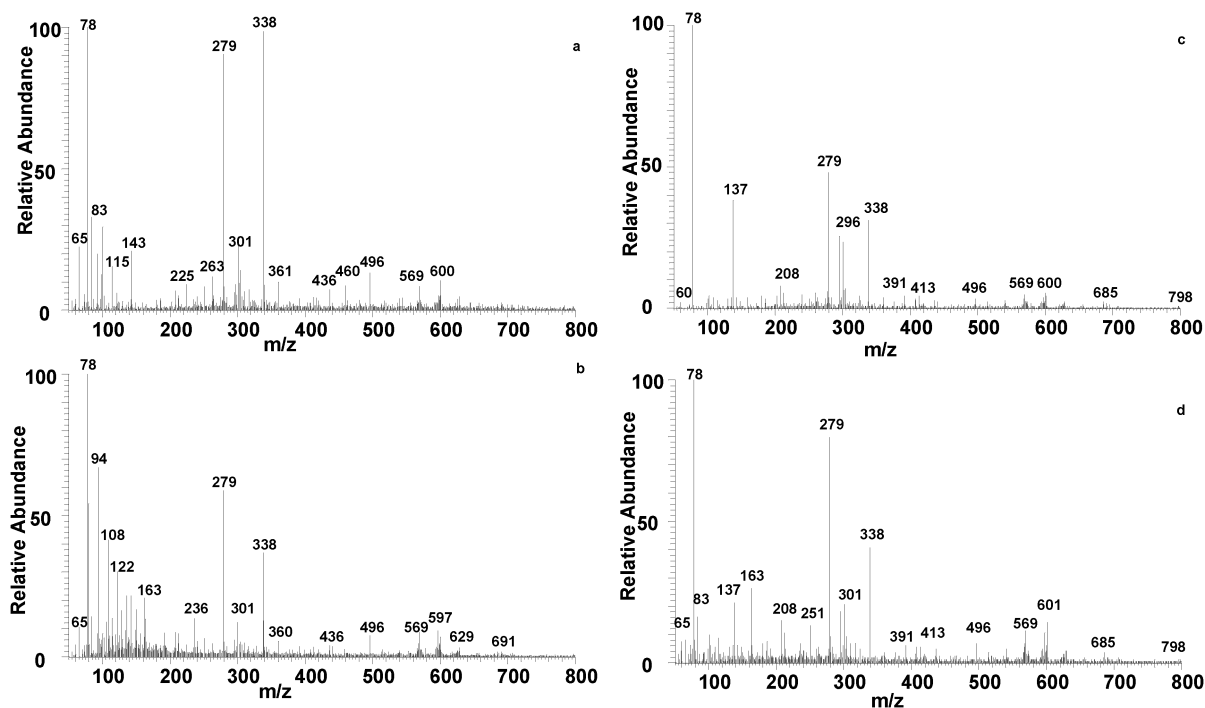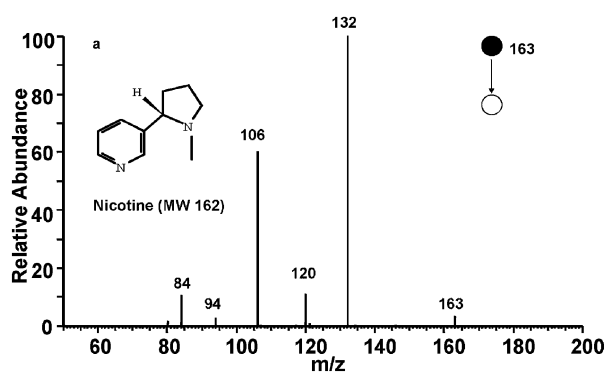
Fig. 5 Mass spectral fingerprints recorded from exhaled breath of different volunteers using EESI-LTQ-MS. The MS spectrum in Fig. 5b was collected 5 min after smoking; and the MS spectrum in Fig. 5d was collected 15 min after smoking.

than that in Fig. 5a. On the other hand, signal levels for peaks such as m/z 83, 263 and m/z 460 decreased significantly, while some peaks such as m/z 78 and m/z 279 maintained almost the same intensities before and after smoking. Note that the time interval between the collections of the two mass spectra was 10 min, part of which (ca. 2 min) was used for smoking. Within such a narrow time window, it is so far hard to tell if the metabolic changes accounted for all the peak alterations. However, the disappeared peaks (e.g., m/z 83, 263 and m/z 460) were most likely eliminated by inhaled smoke in the lung. Similar to the case of the male non-smoker, nicotine was not detectable in the breath of a female non-smoker (shown in Fig. 5c). In the mass spectrum collected in 15 min after she smoked one dose of cigarette (nicotine content was 1.3 mg), the signal of nicotine (m/z 163) was unquestionably detected (shown in Fig. 5d), and was confirmed by using multiple tandem mass spectrometry with data matching of an authentic reference compound. Further, mass spectral peaks observed in Fig. 5d, particularly in the mass range of m/z 50–200, were much more than those observed in the spectrum shown in Fig. 5c. This is consistent with the data obtained with the male volunteer. However, the signal degradation of nicotine was not identical in these two cases. For example, as shown in Fig. 6, the ratio of nicotine signal intensity detected in the female breath to that detected in the male breath varied from 1 : 1 to 3 : 2 and 2 : 1 at 5 min, 10 min and 20 min after her/his smoking, respectively. This ratio increased slowly to reach 3 : 1 in 3 hours in our study. Cotinine, a major metabolite of nicotine, was also detectable in the exhaled breath samples about 1 hour after taking a dose of smoking, showing the similar metabolic dynamics as observed in previous studies.[11] The dynamic responses of nicotine and cotinine shown in Fig. 6 indicate that exhaled breath could be an interesting sample for in vivo pharmacokinetics studies.

Identification of nicotine by tandem mass spectrometry

For most cases where trace amounts of analytes are directly analyzed with complex matrices, MS^n data are usually required for exclusion of false positive signals. Taking the advantage of the ion trap mass analyzer, multiple-stage mass spectrometry experiments can be easily executed with a LTQ-MS instrument. As a demonstration, protonated nicotine molecules (m/z 163) detected from breath samples contributed by a male, regular smoker were used as the precursor ions in this study. In the MS^2 spectrum of nicotine (m/z 163), major fragments of m/z 132 and m/z 106 were recorded upon the CID process with a collision energy of 25% (shown in Fig. 7a). The two characteristic fragments were probably generated by the loss of CH_3NH_2 and $CH_3CH=NCH_3$, respectively. A few small peaks were also observed at m/z 120, 84, 94 and m/z 80. Upon CID, the parent ions of m/z 163 could lose $CH_3CH_2CH_2$ to yield the fragment of m/z 120, which loses HCCH to generate the fragment of m/z 94. The fragment of m/z 84 was produced due to a direct cleavage of neutral C_5NH_5 from the precursor ions (m/z 163). This indicates that the charge stays on the residue of the precursor ion (m/z 163) while a neutral hydrogen atom migrates to the pyridine ring skeleton during the CID process. The tiny peak at m/z 80 could be the protonated pyridine ring, which was generated due to the loss of C_5NH_9 from the precursor ions (m/z 163). The extremely low intensity of the peak at m/z 80 implies that the pathway to generate protonated pyridine is not favored under the experimental conditions. In the MS^3 spectrum, the product ions of m/z 132 yielded major fragments of m/z 117, 115 and m/z 105 (shown in Fig. 7b), probably by the loss of CH_3, NH_3 and HCN, respectively. The relative abundance of m/z 115 (or m/z 105) was
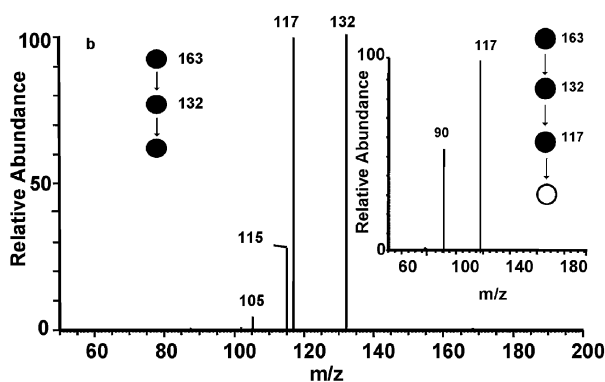

Fig. 6 Plots of the signal intensities of nicotine and cotinine detected in the breath samples donated by the volunteers. The error bars designate 5% of the mean values, which were obtained using 3 measurements for each data point.

Fig. 7 Multiple-stage mass spectrometry data of nicotine detected from the breath sample donated by a regular smoker. (a) the MS^2 spectrum of protonated nicotine (m/z 163); (b) the MS^3 spectrum of nicotine recorded using the product ions of m/z 132 generated in MS^2. The inset shows the MS^4 spectrum recorded using the fragment of m/z 117 generated in the MS^3 experiment.

much lower than that of m/z 117, indicating that the fragmentation path of loss of NH_3 (or HCN) from the precursor ions was not favored. The inset in Fig. 7b shows that the fragment of m/z 117 generated ions of m/z 90 in the MS^4 spectrum by the loss of HCN. No fragment was found from the product ions of m/z 90 in the MS^5 experiment, showing that the product ions of m/z 90 were unlikely to further dissociate under the experimental conditions. The product ions of m/z 106 fragmented into ions of m/z 78 and 79 in the MS^3 spectrum (spectral data not shown), which corresponded to the ring structure of $C_5H_4N^{+\cdot}$ and $C_5H_5N^{+\cdot}$. Note that all the fragmentation paths were confirmed, in terms of both mass-to-charge ratio and relative abundance of the fragments, by using authentic nicotine as a reference compound. In principle, taking the advantage of the LTQ-MS instrument for tandem mass spectrometry, the molecular structures of all the ions detected can be identified by multiple-stage mass spectrometry, plus authentic compounds for reference if necessary.

Semi quantitative analysis of nicotine in breath

For many applications, such as clinical diagnosis and biomarker discovery, it is greatly desirable to obtain quantitative information about the metabolites identified in exhaled breath. As mentioned above, the precursor ions could contain isomers, which might give very similar fragments. To evaluate the signal fraction contributed by other chemicals rather than the analyte to the integrated intensity level, multiple-tandem mass spectrometry experiments are generally required to be done with authentic compounds of the analytes. A good example to eliminate the interference of isomers was demonstrated for direct urine analysis using desorption electrospray ioization ion trap mass spectrometry.[13] In this study, by using authentic nicotine as a reference compound, the same fragmentation patterns of m/z 163 were observed through MS^2 to MS^4 under the same experimental conditions. This confirms that the signal of ions (m/z 163) detected in the breath sample were contributed only by nicotine. This is a key point for quantification of nicotine using the signal detected at m/z 163. If an isomer was suggested by the data of tandem mass spectrometry experiments, it is necessary to use the exclusively characteristic fragments for quantitative analysis. In this study, the calibration curve of nicotine was made
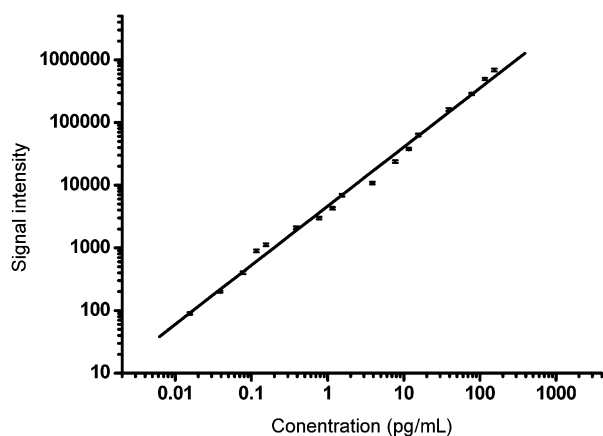

Fig. 8 Calibration curve of nicotine obtained using EESI-LTQ-MS.

Table 2 Analytical results of nicotine concentration in a breath sample

Signal intensity (m/z 163)	Value measured/ pg mL^{-1}	Mean value/pg mL^{-1}	RSD (%)
2.54×10^4, 2.30×10^4, 2.42×10^4, 2.31×10^4, 2.34×10^4, 2.38×10^4, 2.58×10^4, 2.26×10^4, 2.53×10^4, 2.50×10^4	6.1, 5.5, 5.8, 5.5, 5.6, 5.7, 6.2, 5.4, 6.1, 6.0	5.8	5.0

according to the procedure described in the Experimental. It was found that the linear range for nicotine was about 5 orders of magnitude (shown in Fig. 8); and the calibration equation was log y = 0.94228 log c_g (concentration, pg mL^{-1}) + 3.665 with a linearity coefficient R^2 = 0.997 using logarithmic scales. Using the calibration curve, the content of nicotine in the exhaled gas of the male regular smoker was determined to be equivalent to 5.8 pg mL^{-1} in the breath sample analyzed 1 hour after he finished 1 dose of smoking (shown in Table 2). Accordingly, a satisfactory relative standard deviation (RSD) was found to be 5.0% for the nicotine in breath with 10 measurements within 5 min. Under the optimized experimental conditions, the detection limit of nicotine was found to be 0.05 fg mL^{-1} (S/N = 3). Comparing with previous data,[11,13] the LOD (limit of detection) of nicotine was much lower than that obtained using an EESI source implemented in a commercial ESI-QToF-MS instrument. This is because the home-made EESI source was systematically optimized and that the LTQ-MS instrument offers high sensitivity rather than the QToF-MS instrument. Note that the sensitivity of EESI-MS is also compound-dependent. The LOD for compounds of low proton affinity should be much lower than that of nicotine, which has a high proton affinity of 963.4 kJ mol^{-1}.

It is normal for the untrained volunteers to deliver their samples into the Teflon tube using different strengths, *i.e.*, different flow rates. The signal alteration caused by different breath flow rates can be controlled using the flow-rate-regulating valve (shown in Fig. 1). No breath sample passed the valve if the pressure of the sample was lower than the threshold value (*i.e.*, 1.10×10^5 Pa in this study); once the total pressure of the breath sample was more than 1.10×10^5 Pa (*e.g.*, in cases of high flow rates), the volume of the breath sample was expanded rapidly in the ambient air to balance the pressure. Consequently, the breath flow rate was controlled, and the signal alterations of different untrained volunteers generated reasonably low RSD values (<5%) (as shown in Table 3), which were acceptable for trace analysis.

Outcome of EESI-ITMS for breath analysis

Generally, besides the factors such as sensitivity, precision and specificity, other concerns including safety, speed and convenience are important to analytical methods. Mass spectrometry, especially multiple-stage mass spectrometry, is well recognized as a powerful analytical method with high sensitivity, good precision and high specificity. Similar features have been achieved by

Table 3 Reproducible EESI-MS measurements for *in vivo* analysis of breath samples donated by untrained volunteers

Smokers	Signal intensity of nicotine (*m/z* 163, 12 measurements)	Concentration of nicotine/ pg mL^{-1}	Averaged concentration pg mL^{-1}	RSD (%)
1	2.27×10^4, 2.30×10^4, 2.38×10^4, 2.44×10^4, 2.42×10^4, 2.45×10^4, 2.44×10^4, 2.48×10^4, 2.25×10^4, 2.53×10^4, 2.59×10^4, 2.42×10^4	5.4, 5.5, 5.7, 5.8, 5.8, 5.9, 5.8, 5.9, 5.4, 6.1, 6.2, 5.8	5.8	4.2
2	3.21×10^4, 3.11×10^4, 3.18×10^4, 3.39×10^4, 2.82×10^4, 2.99×10^4, 3.05×10^4, 3.32×10^4, 3.15×10^4, 3.03×10^4, 3.10×10^4, 3.19×10^4	7.8, 7.6, 7.7, 8.3, 6.8, 7.3, 7.4, 8.1, 7.7, 7.4, 7.5, 7.8	7.6	4.8

EESI-MS.[11,12,21–23,50,51,55] Taking the advantages of the unique design of the EESI source, living objects (*e.g.*, patients) can be continuously monitored in real-time,[12,23,51] because samples for analysis by EESI-MS are not contaminated by a spray solvent (as in DESI[13,59–62]) or thermally degraded (as in DART[63]), or chemically attacked (as in DAPCI[64,65]). With neutral desorption sampling, biological surfaces can be easily sampled for EESI-MS analysis.[12,21,23,51] Thus, EESI provides ultimate safety for analysis of living objects. Usually, the speed of mass spectrometric analysis is restricted by the sample introduction rather than the mass analysis itself. For most MS instruments, a mass spectrum can be recorded within tens of milliseconds. In this study, because no sample pre-treatment was required, multiple stage (MS^3) tandem mass spectrometry experiments were accomplished within a few seconds. Once the calibration curve is established, EESI-LTQ-MS provides high speed for semi-quantitative *in vivo* breath analysis.

Conclusions

A novel platform based on EESI tandem mass spectrometry was constructed for *in vivo* breath analysis, using a home-made EESI source coupled to a commercially available linear trap quadrupole mass spectrometer. The working conditions of the EESI source were systematically investigated by using *n*-octyl amine as the reference compound. Under the optimized conditions, an LOD was found to be 0.05 fg mL^{-1} ($S/N = 3$, RSD = 5.0%, $n = 8$) for nicotine, with a linear dynamic range of 5 orders of magnitude. Metabolic changes of the human body were rapidly followed by *in vivo* profiling the metabolites in exhaled gas samples donated by several individuals, providing a good agreement with previous studies that exhaled breath can be alternatively used as

a sample for metabolomics studies.[11,32–38,66,67] Nicotine inhaled in the lung, and other metabolites in breath as well, can be promptly identified based on the data obtained using multiple stage tandem mass spectrometry experiments. It is also demonstrated that EESI ion trap mass spectrometry can be used to obtain semi-quantitative information for *in vivo* breath analysis. So far, the accuracy of quantitative analysis is largely controlled by the standard breath sample. The standard nicotine sample used in this study may not exactly be the same as a genuine breath sample, but it is still useful to provide semi-quantitative information of nicotine in exhaled breath. Therefore, the EESI ion trap mass spectrometry is a versatile and practically convenient analytical tool for *in vivo* metabolomics studies.

References

1 A. Aderem, *Cell*, 2005, **121**, 511–513.
2 J. K. Nicholson and J. C. Lindon, *Nature*, 2008, **455**, 1054–1056.
3 L. Hood, J. R. Heath, M. E. Phelps and B. Y. Lin, *Science*, 2004, **306**, 640–643.
4 H. Kitano, *Science*, 2002, **295**, 1662–1664.
5 J. K. Nicholson and I. D. Wilson, *Nat. Rev. Drug Discovery*, 2003, **2**, 668–676.
6 E. C. Butcher, E. L. Berg and E. J. Kunkel, *Nat. Biotechnol.*, 2004, **22**, 1253–1259.
7 R. Russell, *Drug Metab. Rev.*, 2006, **38**, 2–2.
8 G. A. N. Gowda, S. C. Zhang, H. W. Gu, V. Asiago, N. Shanaiah and D. Raftery, *Expert Rev. Mol. Diagn.*, 2008, **8**, 617–633.
9 X. Lu, X. J. Zhao, C. M. Bai, C. X. Zhao, G. Lu and G. M. Xu, *J. Chromatogr. B*, 2008, **866**, 64–76.
10 W. R. Wikoff, J. A. Gangoiti, B. A. Barshop and G. Siuzdak, *Clin. Chem.*, 2007, **53**, 2169–2176.
11 H. Chen, A. Wortmann, W. Zhang and R. Zenobi, *Angew. Chem., Int. Ed.*, 2007, **46**, 580–583.
12 H. Chen, A. Wortmann and R. Zenobi, *J. Mass Spectrom.*, 2007, **42**, 1123–1135.
13 H. Chen, Z. Pan, N. Talaty, D. Raftery and R. G. Cooks, *Rapid Commun. Mass Spectrom.*, 2006, **20**, 1577–1584.
14 P. Forgue, S. Halouska, M. Werth, K. Xu, S. Harris and R. Powers, *J. Proteome Res.*, 2006, **5**, 1916–1923.
15 M. A. Constantinou, A. Tsantili-Kakoulidou, I. Andreadou, E. K. Iliodromitis, D. T. Kremastinos and E. Mikros, *Eur. J. Pharm. Sci.*, 2007, **30**, 303–314.
16 M. Bogdanov, W. R. Matson, L. Wang, T. Matson, R. Saunders-Pullman, S. S. Bressman and M. F. Beal, *Brain*, 2008, **131**, 389–396.
17 E. E. K. Baidoo, P. I. Benket, C. Neususs, M. Pelzing, G. Kruppa, J. A. Leary and J. D. Keasling, *Anal. Chem.*, 2008, **80**, 3112–3122.
18 C. J. Bolten, P. Kiefer, F. Letisse, J. C. Portais and C. Wittmann, *Anal. Chem.*, 2007, **79**, 3843–3849.
19 E. Werner, V. Croixmarie, T. Umbdenstock, E. Ezan, P. Chaminade, J. C. Tabet and C. Junot, *Anal. Chem.*, 2008, **80**, 4918–4932.
20 E. Werner, J. F. Heilier, C. Ducruix, E. Ezan, C. Junot and J. C. Tabet, *J. Chromatogr. B*, 2008, **871**, 143–163.
21 H. Chen, Y. Sun, A. Wortmann, H. Gu and R. Zenobi, *Anal. Chem.*, 2007, **79**, 1447–1455.
22 H. Gu, H. Chen, Z. Pan, A. U. Jackson, N. Talaty, B. Xi, C. Kissinger, C. Duda, D. Mann, D. Raftery and R. G. Cooks, *Anal. Chem.*, 2007, **79**, 89–97.
23 H. Chen, S. Yang, A. Wortmann and R. Zenobi, *Angew. Chem., Int. Ed.*, 2007, **46**, 7591–7594.

24 R. Ramautar, A. Demirci and G. J. de Jong, *TrAC, Trends Anal. Chem.*, 2006, **25**, 455–466.
25 G. Theodoridis, H. G. Gika and I. D. Wilson, *TrAC, Trends Anal. Chem.*, 2008, **27**, 251–260.
26 D. P. Cherney, D. R. Ekman, D. J. Dix and T. W. Collette, *Anal. Chem.*, 2007, **79**, 7324–7332.
27 W. B. Dunn and D. I. Ellis, *TrAC, Trends Anal. Chem.*, 2005, **24**, 285–294.
28 J. C. Lindon and J. K. Nicholson, *TrAC, Trends Anal. Chem.*, 2008, **27**, 194–204.
29 H. M. G. Pereira, M. C. Padilha, R. M. A. Bento, T. P. Cunha, N. A. G. Lascas and F. R. A. Neto, *TrAC, Trends Anal. Chem.*, 2008, **27**, 648–656.
30 M. Thevis, H. Geyer, U. Mareck, G. Sigmund, J. Henke, L. Henke and W. Schanzer, *Anal. Bioanal. Chem.*, 2007, **388**, 1539–1543.
31 M. Giardina and S. V. Olesik, *Anal. Chem.*, 2003, **75**, 1604–1614.
32 D. H. Conrad, J. Goyette and P. S. Thomas, *J. Gen. Intern. Med.*, 2008, **23**, 78–84.
33 S. A. Kharitonov and P. J. Barnes, *Chest*, 2006, **130**, 1541–1546.
34 C. A. Wyse, T. Preston, P. S. Yam, D. G. M. Sutton, R. M. Christley, J. W. Hotchkiss, C. A. Mills, A. Glidle, D. R. S. Cumming, J. M. Cooper and S. Love, *Vet. Rec.*, 2004, **154**, 353–362.
35 P. Martínez-Lozano and J. F. n. d. l. Mora, *Anal. Chem.*, 2008, **80**, 8210–8215.
36 W. Ma, X. Y. Liu and J. Pawliszyn, *Anal. Bioanal. Chem.*, 2006, **385**, 1398–1408.
37 S. Carraro, S. Rezzi, F. Reniero, K. Heberger, G. Giordano, S. Zanconato, C. Guillou and E. Baraldi, *Am. J. Respir. Crit. Care. Med.*, 2007, **175**, 986–990.
38 F. Hoffmeyer, V. Harth, R. Merget, N. Goldscheid, E. Heinze, P. Degens, B. Pesch, J. Bunger, T. Bruning and M. Raulf-Heimsoth, *J. Physiol. Pharmacol.*, 2007, **58**, 289–298.
39 A. Conventz, A. Musiol, C. Brodowsky, A. Mueller-Lux, P. Dewes, T. Kraus and T. Schettgen, *J. Chromatogr. B*, 2007, **860**, 78–85.
40 K. Czebe, I. Barta, B. Antus, M. Valyon, I. Horvath and T. Kullmann, *Respir. Med.*, 2008, **102**, 720–725.
41 A. Koutsokera, S. Loukides, K. I. Gourgoulianis and K. Kostikas, *Curr. Med. Chem.*, 2008, **15**, 620–630.
42 Z. L. Borrill, K. Roy and D. Singh, *Eur. Respir. J.*, 2008, **32**, 472–486.
43 L. Keck, C. Hoeschen and U. Oeh, *Int. J. Mass Spectrom.*, 2008, **270**, 156–165.
44 M. Norman, A. Hansel and A. Wisthaler, *Int. J. Mass Spectrom.*, 2007, **265**, 382–387.
45 W. Q. Cao and Y. X. Duan, *Crit. Rev. Anal. Chem.*, 2007, **37**, 3–13.
46 P. Spanel, K. Dryahina and D. Smith, *Int. J. Mass Spectrom.*, 2006, **249–250**, 230–239.
47 D. Smith, T. S. Wang, A. Pysanenko and P. Spanel, *Rapid Commun. Mass Spectrom.*, 2008, **22**, 783–789.
48 C. Turner, B. Parekh, C. Walton, P. Spanel, D. Smith and M. Evans, *Rapid Commun. Mass Spectrom.*, 2008, **22**, 526–532.
49 D. Smith and P. Spanel, *Analyst*, 2007, **132**, 390–396.
50 H. Chen, A. Venter and R. G. Cooks, *Chem. Commun.*, 2006, 2042–2044.
51 H. Chen and R. Zenobi, *Nat. Protoc.*, 2008, **3**, 1467–1475.
52 H. Chen, D. Touboul, M. C. Jecklin, J. Zheng, M. Luo and R. Zenobi, *Eur. J. Mass Spectrom.*, 2007, **13**, 273–279.
53 K. Chingin, G. Gamez, H. Chen, L. Zhu and R. Zenobi, *Rapid Commun. Mass Spectrom.*, 2008, **22**, 2009–2014.
54 Y. M. Zhou, J. H. Ding, X. Zhang and H. W. Chen, *Chin. Chem. Lett.*, 2007, **18**, 115–117.
55 Z. Zhou, M. Jin, J. Ding, Y. Zhou, J. Zheng and H. Chen, *Metabolomics*, 2007, **3**, 101–104.
56 L. B. Norton, C. R. Bigelow, and W. B. Vincent, *J. Am. Chem. Soc.*, 1940, **62**, 261–264.
57 P. J. Lipowicza and J. Piadé, *J. Aerosol Sci.*, 2004, **35**, 33–45.
58 B. K. Pramanik, A. K. Gangoly, M. L. Gross, *Applied Electrospray Mass Spectrometry*, Marcel Dekker Inc., New York, 2002.
59 E. H. Seeley and R. M. Caprioli, *Proteomics: Clin. Appl.*, 2008, **2**, 1435–1443.
60 X. J. Feng, X. Liu, Q. M. Luo and B. F. Liu, *Mass Spectrom. Rev.*, 2008, **27**, 635–660.
61 H. W. Chen, N. N. Talaty, Z. Takats and R. G. Cooks, *Anal. Chem.*, 2005, **77**, 6915–6927.
62 Z. Takáts, J. M. Wiseman and R. G. Cooks, *J. Mass Spectrom.*, 2005, **40**, 1261–1275.
63 R. B. Cody, J. A. Laramée and H. D. Durst, *Anal. Chem.*, 2005, **77**, 2297–2302.
64 H. Chen, J. Zheng, X. Zhang, M. Luo, Z. Wang and X. Qiao, *J. Mass Spectrom.*, 2007, **42**, 1045–1056.
65 S. Yang, J. Ding, L. Zhu, B. Hu, J. Li, H. Chen, Z. Zhou and X. Qiao, *Anal. Chem.*, 2009, **81**, 2426–2436.
66 H. Lord, Y. Yu, A. Segal and J. Pawliszyn, *Anal. Chem.*, 2002, **74**, 5650–5657.
67 L. C. A. Amorim and Z. D. L. Cardeal, *J. Chromatogr. B*, 2007, **853**, 1–9.